

Magneto-optical properties of Fe-Pt alloy films in the range 1.55–10.5 eV

Toshio Sugimoto*

College of Science and Technology, Nihon University, Funabashi, Chiba 274, Japan

Toshikazu Katayama and Yoshishige Suzuki†

Electrotechnical Laboratory, Tsukuba, Ibaraki 305, Japan

Tsuneharu Koide and Tetsuo Sidara

Photon Factory, National Laboratory for High Energy Physics, Tsukuba, Ibaraki 305, Japan

Masatada Yuri‡

Institute of Physics, University of Tsukuba, Tsukuba, Ibaraki 305, Japan

Akiyoshi Itoh and Kenji Kawanishi

College of Science and Technology, Nihon University, Funabashi, Chiba 274, Japan

(Received 10 June 1993)

The optical and magneto-optical properties of as-deposited and annealed Fe₅₁Pt₄₉ films were investigated in the photon energy range 1.55–10.5 eV. The magneto-optical Kerr rotation (θ_K) spectra of both films were found to show a dispersion-type structure in the 4.6–7.8 eV region: they have large negative and broad positive peaks at around 4.8 and 7.8 eV, respectively. The θ_K spectra showed a tendency that is essentially quite similar to that of bulk Fe. The Kerr ellipticity (η_K) spectra are bell shaped, exhibiting a large negative peak at 6.3 eV. Plasma edges were observed at 6.9 eV for the as-deposited film and at 7.3 eV for the annealed film. The absolute value of the real part of the off-diagonal dielectric element (ϵ'_{XY}) of both films at ~ 4.8 eV are almost the same as that of bulk Fe. This leads to the conclusion that the θ_K enhancement at 4.8 eV is mainly due to a decrease in ϵ'_{XX} and a peak shift in ϵ'_{XY} towards lower energy, but not to a plasma-resonance effect.

I. INTRODUCTION

Large magneto-optical Kerr rotation and a perpendicular magnetic anisotropy are required for applications to high-density magneto-optical (MO) recording media. Much attention has recently been focused on 3d-ferromagnetic transition metals/(Pt,Pd) multilayers, since they have the possibility to be a next generation MO recording medium.^{1–5} In those multilayers, new MO effects and magnetic anisotropy caused by induced moments in Pt and Pd atoms are expected from the points of view of both basic research and applications.^{6,7}

We investigated the magneto-optical Kerr effect and the perpendicular magnetic anisotropy in Fe/Pt and Co/Pt multilayers as well as their alloy films.^{5,8} It has been reported that the magneto-optical Kerr rotation (θ_K) is considerably enhanced at 4.8 and 4.0 eV in Fe/Pt and Co/Pt multilayers, respectively.^{2–5} Concerning the θ_K enhancement in Co/Pt multilayers, Moog, Zak, and Bader¹⁰ pointed out that the observed MO peak at 4.0 eV cannot be explained by the virtual optical constant method using the optical constants of bulk metals.

On the other hand, the θ_K spectra of the (Co,Fe)/(Pt,Pd) multilayers resemble those of alloy films which have the same composition as the multilayers.^{5,9} From these results, the θ_K enhancements have been attributed to alloyed layers at the interfaces.^{4,7,10–12} For Co-Pt and Co-Pd alloys, Buschow, van Ergen, and Jonge-

breur⁹ reported Kerr enhancements at around 4.0 and 3.5 eV, respectively. Weller *et al.*^{7,12} showed that those energies are coincident with the binding energies of the *d* bands of Pt and Pd in alloys with Co, attributing the Kerr enhancement to the transitions from the *d* bands of Pt and Pd to the *s,p* bands just above the Fermi level. However, Reim *et al.*¹³ suggested a dispersion-type contribution of Pd atoms in Fe-Pd alloys, which was centered at 1.9 eV, since Pd not only has a contribution at around 4.0 eV, but also a negative contribution to the Kerr rotation at around 1.9 eV. Thus, many researchers have expected so far that the spin-polarized Pt and Pd atoms adjacent to the 3d-transition metals may be responsible for the θ_K enhancement. However, so far there has been no conclusive agreement concerning the contribution of Pt and Pd on the MO effect.

The role played by Fe and Co atoms in the MO effect in the (Fe,Co)/(Pt,Pd) multilayers and alloys has not been discussed, though the electronic structures of Fe and Co should be changed upon alloying; those atoms are expected to have characteristic contributions to the MO effect. In general, the orbital and spin magnetic moments largely contribute to the MO effects.¹⁴ Those of 3d-transition metals strongly depend on the atomic coordination number,⁶ the spin-orbit interaction on *d* electrons,¹⁵ and the symmetry of *d*-wave functions¹⁶ in binary 3d-metal alloys. It is of interest to study whether the orbital and spin magnetic moments of Fe or Co in their alloys are

enhanced or not.

To investigate the contributions of Fe, Co, Pt, and Pd to the MO effects in those alloys, it is important to measure the MO spectra over a wide photon energy range. Since the valence-band width of metal alloys including Fe or Co is about 10 eV,^{7,12,13} a MO measurement in a range at least up to 10 eV is required in order to clarify the contribution of the band-to-band transitions responsible for the MO effect. As far as we know, however, few experimental studies have been reported¹⁷ concerning MO effects in the vacuum ultraviolet region (beyond about 6.0 eV). The main reason is that above 6.0 eV the absorption of quartz optical devices used in a MO apparatus is high and a high-vacuum-compatible magnet system is required. It is difficult to study the MO effect in detail without any measurements of the optical and MO spectra over a wide energy range.

Fe-Pt alloys near 50 at. % Pt have disordered and ordered crystal phases, and the magnetic properties are different for each crystal phase.^{18,19} It is thus expected that the electronic structure and the contribution of Pt atoms to the MO effect are probably different for the two phases. Therefore, it is also interesting to compare the MO properties of the two phases.

In this paper we report on the optical and MO properties of as-deposited and annealed Fe₅₁Pt₄₉ films within the energy range 1.55–10.5 eV. The measurements were made using a Xe lamp and synchrotron radiation (SR). The diagonal and off-diagonal dielectric elements (ϵ_{XX} and ϵ_{XY}) of those films are also presented as a function of the photon energy. The origin of the θ_K enhancement at 4.8 eV in Fe₅₁Pt₄₉ films is discussed in terms of ϵ_{XX} and ϵ_{XY} .

II. EXPERIMENTAL PROCEDURES

All Fe₅₁Pt₄₉ films were prepared onto a quartz substrate by means of a rf sputtering method using a tip-on-target. The base pressure of the vacuum chamber was below 5×10^{-8} Torr and the Ar pressure was 20 m Torr during sputtering. The purity of the raw materials was 99.95% for Fe and 99.99% for Pt. To obtain an as-deposited (disordered) alloy sample, the substrate was maintained at about 20°C by water cooling during film deposition. The annealed (ordered) film was prepared at about 380°C and kept at 380°C for 2 h in the same chamber, evacuated to less than 2×10^{-7} Torr. After the film preparation, the surfaces of the alloy films were overcoated with a Pt layer with a thickness of 10 Å in order to prevent the film from oxidization.

The crystal structure was examined by the x-ray-diffraction (XRD) method. Co-K α ($\lambda = 1.7902$ Å) radiation was used as an x-ray source. The composition of the films was determined by an electron probe microanalyser.

The magnetic circular dichroism (MCD) and reflectivity (R) spectra were measured in the regions 4.0–10.5 and 4.0–40.0 eV, respectively, using SR on beamline BL-11C of the Photon Factory, National Laboratory for High Energy Physics. A schematic diagram of the MCD measurement is shown in Fig. 1; the optical system for conveying the SR and the arrangement of the

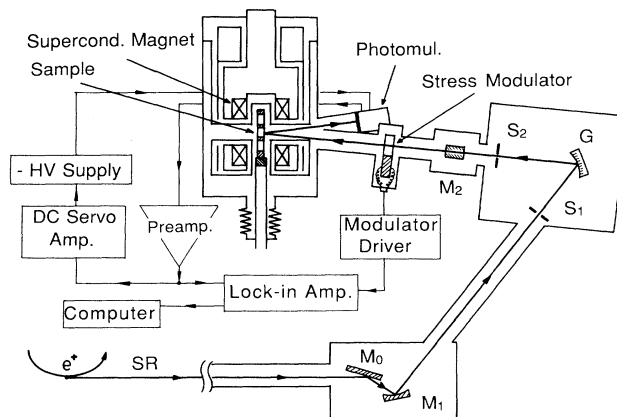


FIG. 1. Arrangement for the MCD experiment on Seya-Namioka beamline (BL-11C) (Ref. 20). Linearly polarized SR is converted to circularly polarized SR with a LiF photoelastic modulator. M_0 is the plane mirror for vertical deflection; M_1 the spherical mirror; M_2 the toroidal mirror; S_1 the entrance slit; S_2 the exit slit; and G the grating. The sample was placed at the center of a split-type UHV 5.8-T superconducting magnet (Ref. 21).

MCD experiment were previously reported in detail.^{20,21} The measurements were carried out under a high vacuum in the 10^{-9} Torr range. The MCD spectra were taken using a polarization modulation technique with a light incidence angle of 4°. A LiF photoelastic modulator was used as a polarization modulator. The external magnetic field was varied up to 5 T, depending on the saturation fields of the samples.

The reflection MCD spectrum corresponds to the difference (ΔR) in the reflectivities for left (R_+) and right (R_-) circularly polarized light. Since ΔR is proportional to the ac output current (I_{ac}) of the photomultiplier tube, and its dc output current (I_{dc}) was kept constant, the ratio of ΔR to the average reflectivity (R) can be deduced as

$$\Delta R / R \propto I_{ac} / I_{dc} , \quad (1)$$

where $\Delta R = R_+ - R_-$ and $R = (R_+ + R_-) / 2$. The Kerr ellipticity (η_K) is related to the MCD signal by

$$\eta_K = \frac{1}{4} (\Delta R / R) . \quad (2)$$

The θ_K spectrum can be derived from the η_K spectrum by a Kramers-Kronig (KK) transformation.

The θ_K spectrum was also measured with a Kerr rotation spectrometer (Jasco J-250) from 250 to 800 nm (5.3–1.55 eV). The η_K spectrum was calculated from the measured θ_K spectrum using a KK transformation. The maximum magnetic field was 1.5 T. The light incidence angle was 10° with respect to the surface normal. The reflectivity was measured using a spectrophotometer (Jasco 660) from 200 to 900 nm (6.2–1.4 eV).

III. EXPERIMENTAL RESULTS

A. Film structure

Figures 2(a) and 2(b) show the x-ray-diffraction patterns of as-deposited and annealed $\text{Fe}_{51}\text{Pt}_{49}$ films, respectively. From Fig. 2(a), it has been confirmed that the as-deposited film has a stacking of close-packed (111) atomic planes of the face-centered-cubic (fcc) structure. No diffraction lines indicating other crystal structures were detected. On the other hand, Fig. 2(b) exhibits several superlattice lines, such as (001), (110), (112), and (022), corresponding to the face-centered-tetragonal (fct) structure in addition to a fundamental (111) line. Since the intensities of the superlattice lines hardly changed upon further annealing at higher temperatures, the film had presumably an ordered phase due to *in situ* annealing. Hereafter, the as-deposited and annealed $\text{Fe}_{51}\text{Pt}_{49}$ films are referred to as disordered and ordered films, respectively.

B. Magneto-optical spectra in the range 1.55–10.5 eV

Figure 3(a) shows the θ_K and η_K spectra of $\text{Fe}_{51}\text{Pt}_{49}$ films. The theoretical θ_K spectrum of bulk Fe is displayed for a comparison.²² Here, the η_K spectra were deduced from the θ_K spectra by a KK transformation. Since the θ_K data have not been extrapolated beyond the measured energy range in the KK transformation, η_K may have some errors at both ends of the range. The θ_K and η_K spectra of several Fe/Pt multilayers are also shown in Fig. 3(b) for a comparison. The θ_K spectrum is essentially identical for the alloy films and multilayers.

Comparing the θ_K spectra of both alloy films with that of bulk Fe shows that θ_K is largely enhanced at 4.8 eV in

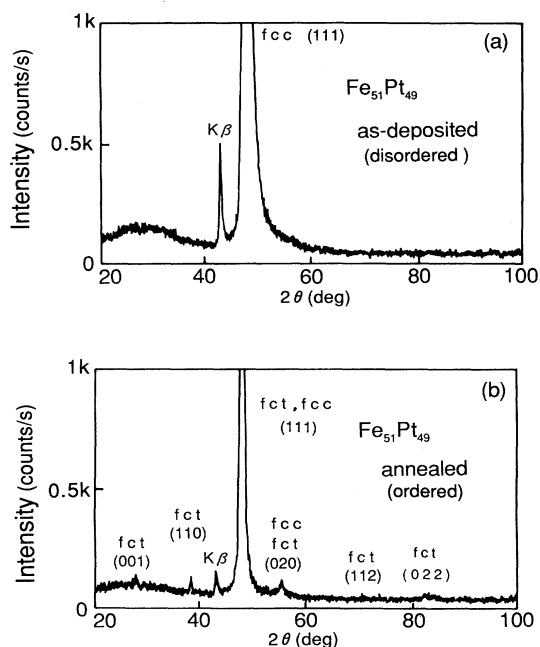


FIG. 2. Wide-angle x-ray-diffraction patterns of (a) as-deposited and (b) annealed $\text{Fe}_{51}\text{Pt}_{49}$ films.

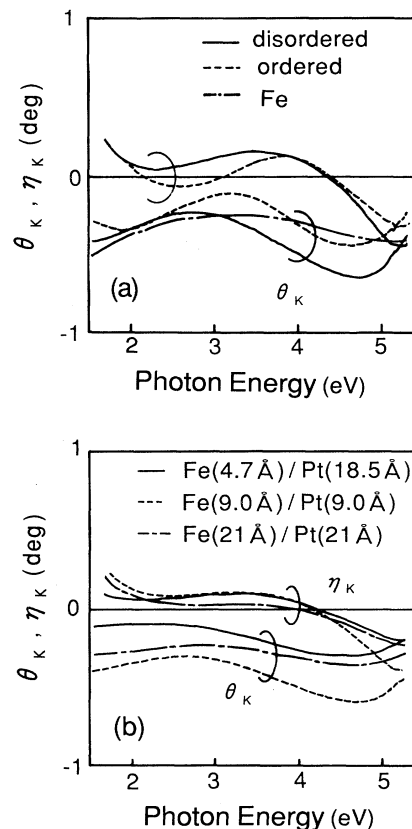


FIG. 3. Kerr rotation (θ_K) and Kerr ellipticity (η_K) spectra (a) for disordered and ordered $\text{Fe}_{51}\text{Pt}_{49}$ films and (b) for several Fe/Pt multilayers from 1.55 to 5.3 eV. A calculated θ_K spectrum of bulk Fe is shown for comparison (Ref. 22). From the XRD measurement, it was confirmed that all multilayers have a stacking of close-packed atomic layers and a periodic structure along the normal to the film surface.

the alloys, and that the absolute value of θ_K below about 3.0 eV is smaller for the alloys than for bulk Fe. The absolute magnitude of θ_K of the ordered film is less than that of the disordered film over the entire energy range. A new peak appears at ~ 2.0 eV for the ordered film.

Figure 4 shows the reflection MCD spectra ($\Delta R/R$) for the disordered and ordered films from 4.0 to 10.5 eV. The errors are mainly due to the phase shift between the ac voltage applied to the photoelastic modulator and the detected ac output current of the photomultiplier tube. The errors below about 6 eV may arise from a mixing of second-order light. The errors above about 10 eV are caused by the decreased transmittance of LiF. The MCD spectra show a similar tendency for the disordered and ordered films; the MCD spectra of the films have a large negative peak at 6.3 eV and a positive one at ~ 9.5 eV. The MCD spectrum for the ordered film lies above that for the disordered one.

From the data given in Figs. 3(a) and 4, we obtained the θ_K and η_K spectra shown in Figs. 5(a) and 5(b), respectively. The theoretical θ_K spectrum of bulk Fe is displayed in the figures for a comparison.²² The absolute

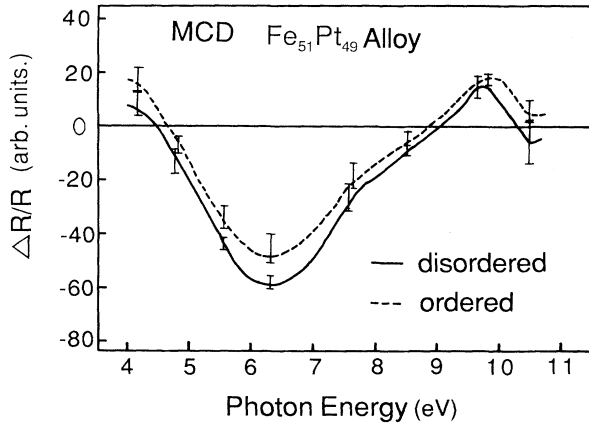


FIG. 4. Magnetic circular dichroism spectra for disordered and ordered $\text{Fe}_{51}\text{Pt}_{49}$ films from 4.0 to 10.5 eV. The surfaces of both films were overcoated with a Pt layer with a thickness of about 10 Å in order to prevent the films from oxidation.

value of θ_K obtained from the MCD was normalized at 4.8 eV to the θ_K value measured with J-250. The reason is as follows: the difference in the peak position near 5.0 eV in the θ_K spectra obtained by two methods is presumably mainly due to a mixing of second-order light in the MCD measurement. If the influence of second-order light is taken into account, the peak in the θ_K spectrum

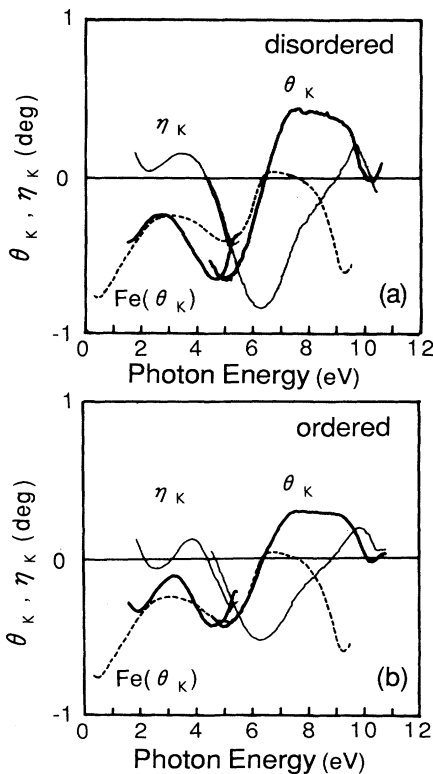


FIG. 5. Kerr rotation (θ_K) and Kerr ellipticity (η_K) spectra for (a) the disordered and (b) the ordered $\text{Fe}_{51}\text{Pt}_{49}$ films from 1.55 to 10.5 eV. The calculated result (Ref. 22) for bulk Fe is indicated by a dotted curve.

obtained from the MCD data should shift to lower energy. Hence, the negative θ_K peak at 5.2 eV resulting from the MCD data should naturally be conceived to coincide in energy with that at 4.8 eV, resulting from the J-250 data.

The entire θ_K and η_K spectra show a similar tendency for the disordered and ordered films, except for a structure at ~ 2.0 eV. Namely, the θ_K spectrum has a large negative peak at 4.8 eV and a broad positive structure from 7.0 to 9.5 eV for both films. The η_K spectrum exhibits a large negative peak at 6.3 eV and a feature at ~ 9.5 eV. However, the absolute values of θ_K and η_K are larger for the disordered film than for the ordered one. Both η_K show bell-shaped spectra with a center energy of 6.3 eV; the θ_K spectra from 4.8 to 7.6 eV exhibit a dispersion-type shape centered at 6.3 eV. The θ_K spectrum of bulk Fe seems to have a dispersion centered at 5.9 eV.²² This behavior is very similar to that of the $\text{Fe}_{51}\text{Pt}_{49}$ films.

C. Diagonal dielectric element (ϵ_{XX}) deduced from a reflectivity measurement

Figure 6 shows the reflectivity (R) spectra of the disordered and ordered films. Both spectra show a tendency to decrease monotonically with increasing photon energy. The absolute value of R is higher for the ordered film than for the disordered film. A maximum in R is observed at ~ 23 eV for both films. For the ordered film, features are seen at ~ 4 , ~ 9 , and ~ 15 eV. Since Seignac and Robin reported a maximum in R at ~ 24 eV in a Pt film,²³ the peaks at ~ 23 eV in our spectra are conceivably related with the characteristic structure of Pt.

In general, the refractive index (n) and the extinction coefficient (k) can be derived from the reflectivity (R) and the phase angle (Θ) by²⁴

$$n = (1 - R) / (1 + R - 2\sqrt{R} \cos\Theta) \quad (3a)$$

and

$$k = (2\sqrt{R} \sin\Theta) / (1 + R - 2\sqrt{R} \cos\Theta) . \quad (3b)$$

$\Theta(h\nu)$ was calculated from $R(h\nu)$ using a KK transformation. For the KK analysis, $R(h\nu)$ was extrapolated to

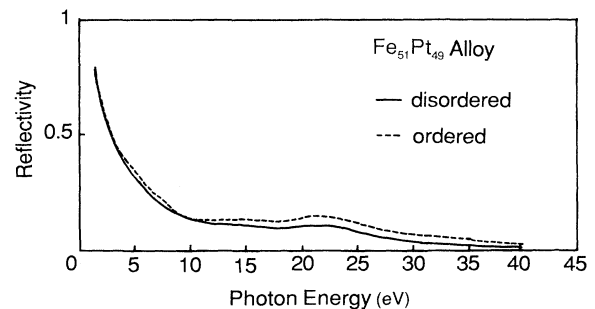


FIG. 6. Reflectivity (R) spectra for the disordered and ordered $\text{Fe}_{51}\text{Pt}_{49}$ films from 1.4 to 40.0 eV. The surface of both films was overcoated with a Pt layer with a thickness of about 10 Å in order to prevent the films from oxidation.

lower and higher energies under the assumption of a free-electron asymptotic limit.²⁵

The real (ϵ'_{XX}) and imaginary (ϵ''_{XX}) parts of the diagonal element (ϵ_{XX}) of the complex dielectric tensor are related to n and k by $\epsilon'_{XX} = n^2 - k^2$ and $\epsilon''_{XX} = 2nk$. The ϵ'_{XX} and ϵ''_{XX} spectra of the disordered and ordered films are shown in Fig. 7 in the energy range from 1.55 to 11.5 eV. The theoretical and experimental spectra of bulk Fe are also shown for a comparison.^{22,26} The ϵ'_{XX} and ϵ''_{XX} spectra of both alloy films resemble each other. ϵ'_{XX} monotonically increases with the photon energy, crossing the abscissa at 6.9 eV for the disordered film and at 7.3 eV for the ordered one. This indicates that these energies are the plasma edges of the films. In contrast, the ϵ''_{XX} decreases with the photon energy. Although there are several features in the R spectrum of the ordered film (Fig. 6), no corresponding structures can be clearly seen in the ϵ'_{XX} and the ϵ''_{XX} spectra.

Comparing the ϵ'_{XX} and ϵ''_{XX} spectra of the $\text{Fe}_{51}\text{Pt}_{49}$ films with those of bulk Fe, their absolute values are smaller for the alloy films than for bulk Fe below about 7.0 eV. The structure in ϵ'_{XX} and ϵ''_{XX} observed for bulk Fe in the range 1.5–4.0 eV diminishes in the alloy films. In the region from 4.0 to 7.0 eV, where θ_K (or η_K) enhancement was observed, the ϵ'_{XX} and ϵ''_{XX} spectra of the disordered and ordered films are similar to each other, except for their absolute magnitude.

D. Off-diagonal dielectric element (ϵ_{XY}) deduced from the optical and the magneto-optical measurements

The real (ϵ'_{XY}) and imaginary (ϵ''_{XY}) parts of the off-diagonal element (ϵ_{XY}) of the complex dielectric tensor can be related to n , k , θ_K , and η_K as²⁴

$$\epsilon'_{XY} = -\alpha\theta_K + \beta\eta_K \quad (4a)$$

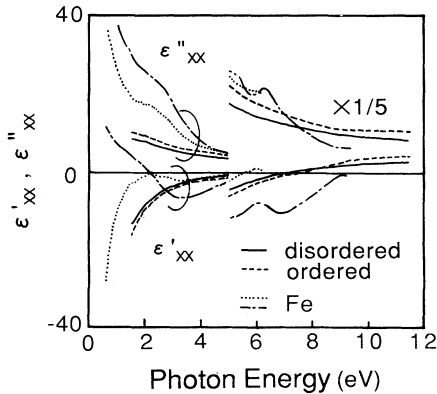


FIG. 7. Real (ϵ'_{XX}) and imaginary (ϵ''_{XX}) parts of the complex diagonal dielectric element (ϵ_{XX}) for the disordered and ordered $\text{Fe}_{51}\text{Pt}_{49}$ films. The spectra of bulk Fe, which were theoretically obtained by Oppenher *et al.* (Ref. 22) (a dash-dotted curve) and experimentally obtained by Johnson *et al.* (Ref. 26) (a dotted curve), are also shown for comparison. A Drude term was not taken into account in the calculation of Ref. 22.

and

$$\epsilon''_{XY} = -\beta\eta_K + \alpha\theta_K, \quad (4b)$$

where α and β are given by

$$\alpha = n(n^2 - 3k^2 - 1) \quad (5a)$$

and

$$\beta = k(3n^2 - k^2 - 1). \quad (5b)$$

Figures 8(a) and 8(b) show the ϵ'_{XY} and ϵ''_{XY} spectra for the disordered and ordered $\text{Fe}_{51}\text{Pt}_{49}$ films, respectively. Those spectra of bulk Fe, obtained theoretically by Oppenher and co-workers,²² are shown for a comparison. They are qualitatively in agreement with the experimental result obtained for an Fe (100) film on Ag by Hayashi *et al.* in the common region.²⁷ However, the absolute value of the theoretical spectra is 1.2 times as large as that of the experimental ones.

The ϵ'_{XY} and ϵ''_{XY} spectra of the disordered film show a tendency similar to those of the ordered film. The ϵ'_{XY} spectra of both films exhibit a dispersion-type shape centered at 6.3 eV. The ϵ''_{XY} spectra show a broad negative peak at 6.3 eV and a feature near 9.5 eV, as do the ϵ'_{XY} spectra. The behavior of ϵ'_{XY} of both films between 4.6 and 7.8 eV is similar to that of bulk Fe, which shows a

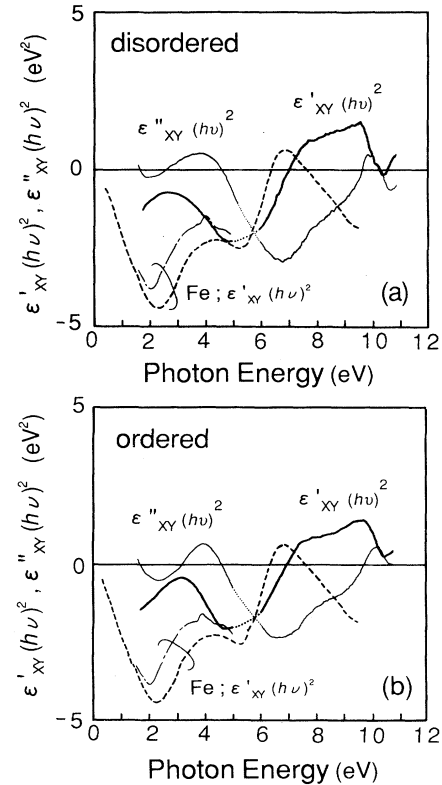


FIG. 8. Real (ϵ'_{XY}) and imaginary (ϵ''_{XY}) parts of the complex off-diagonal dielectric element (ϵ_{XY}) for (a) the disordered and (b) the ordered $\text{Fe}_{51}\text{Pt}_{49}$ films. The spectra of bulk Fe, obtained by Oppenher *et al.* (Ref. 22) (a dotted curve) and Hayashi *et al.* (Ref. 27) (a dash-dotted curve), are also shown for comparison.

dispersion centered at 5.9 eV, although the center energy is different by 0.4 eV.

The amplitude of the dispersion for the alloy films is almost the same as that for bulk Fe. This implies that the dispersion amplitude of ϵ'_{XY} per Fe atom in the $\text{Fe}_{51}\text{Pt}_{49}$ films are about twice that of bulk Fe, if the contributions of Pt atoms are neglected. The dispersion width is about 2.8 eV, being 1.2 eV wider than that of bulk Fe. This arises from the fact that a negative peak at 5.2 eV and a positive one at 6.8 eV for bulk Fe shift to lower and higher energies, respectively, in the alloy films. This result suggests that the feature at around 6.3 eV in the $\text{Fe}_{51}\text{Pt}_{49}$ films may be explained as a diamagnetic-type interband transition.

On the other hand, a large negative peak at ~ 2.0 eV in the ϵ'_{XY} spectrum of bulk Fe disappeared in those of both $\text{Fe}_{51}\text{Pt}_{49}$ films. Comparing the ϵ'_{XY} spectrum of the disordered film with that of the ordered one shows differences in the 2.0–3.5 eV region.

IV. DISCUSSION

A. Magneto-optical effects represented by the dielectric elements

It is well known that the polar Kerr effect in homogeneous systems depends on both the diagonal and the off-diagonal dielectric elements. For normal incidence of light, the complex Kerr rotation, $\Phi_K = \theta_K + i\eta_K$, is expressed as¹⁴

$$\Phi_K = \epsilon_{XY} / \{ (1 - \epsilon_{XX}) \sqrt{\epsilon_{XX}} \}. \quad (6)$$

This suggests the possibility that the Kerr rotation could become large if the denominator is small.²⁸ Namely, a large resonancelike enhancement in θ_K and η_K is expected near the plasma edges where ϵ'_{XX} is equal to zero.

In the $\text{Fe}_{51}\text{Pt}_{49}$ alloys, a θ_K enhancement was observed at 4.8 eV (Fig. 5). However, this energy does not correspond to the plasma edges at 6.9 and 7.3 eV of these alloy films (Fig. 7). In order to examine the contribution of the plasma-resonance effect, the denominator in Eq. (6) was computed for the alloy films. The absolute magnitude of the denominator was found to decrease monotonically with the photon energy, and no drastic change was observed at 4.8 eV. This result shows that the absolute value of Φ_K for the alloy films gradually increases with the photon energy if the value of ϵ_{XY} is constant. Therefore, the appearance of the new peak in θ_K (or η_K) at 4.8 eV (or 6.3 eV) cannot be explained by the plasma-resonance effect in the Fe-Pt alloy systems.

As can be seen in Fig. 8, the values of the ϵ'_{XY} for both alloy films at 4.8 eV, where the θ_K is enhanced, are almost the same as that for bulk Fe, and the negative peak in ϵ'_{XY} for the alloys shifts to lower energy relative to that for bulk Fe. Although the appearance of the θ_K peak at 4.8 eV seems to be due to the peak shift, the θ_K enhancement, itself, is explained phenomenologically by a decrease in ϵ'_{XX} at this energy (Figs. 5 and 7) as well as by an increase in ϵ'_{XY} per Fe atom.

B. Diagonal and off-diagonal dielectric elements

It has been reported that the spin moment of Fe is enhanced and a magnetic moment is induced in Pt or Pd atoms by the proximity effect in their alloys.^{15,29,30} We have verified an enhancement of the saturation magnetization (M_s) from M_s measurements of the Fe-Pt alloys; Fig. 9 shows the M_s measured at 5 K and room temperature as a function of the Pt content. At room temperature, there is about a 10% difference of M_s between the disordered film and the ordered one at 50 at. % Pt. The difference of M_s is mainly considered to originate from a change in the spin magnetic moment of Fe. We have also found that the orbital moment of Fe is enhanced in $\text{Fe}_{51}\text{Pt}_{49}$ films from a core-level MCD experiment.³¹ Table I shows the orbital and spin moments of Fe, Pt, and Pd in

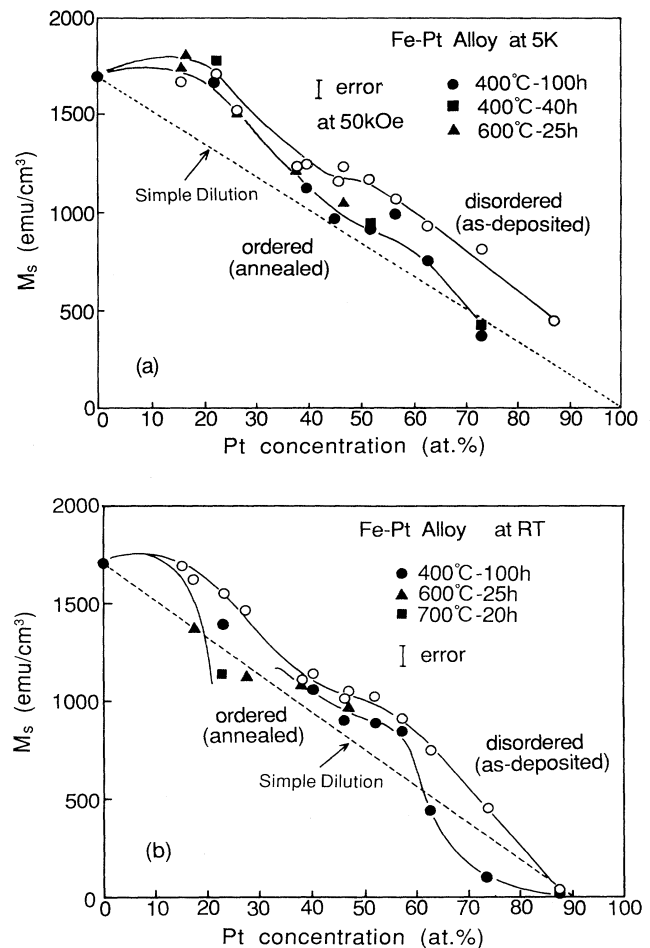


FIG. 9. Saturation magnetization (M_s) as a function of the Pt content measured at (a) 5 K and (b) room temperature (RT) for the Fe-Pt alloy systems. The open and solid-symbols indicated the M_s for the disordered and the ordered alloy films, respectively. The dotted line corresponds to the value of the simple dilution of bulk Fe. The rapid decreases of M_s for the ordered alloy films near 25 at. % Pt are due to the invar effect. The measurements were made with a superconducting quantum interference device (SQUID) equipment. Annealing was carried out in pure H_2 gas using an electric furnace.

TABLE I. Orbital and spin magnetic moments (in μ_B) of Fe, Pt, and Pd in bulk Fe and their alloys.

		$M_{\text{spin}}(\mu_B)$	$M_{\text{orbital}}(\mu_B)$
Fe ^a		2.083	0.0918
Fe ₅₀ Pt ₅₀ ^b	Fe	2.91	0.13
	Pt	0.34	0.07
Fe ₅₀ Pd ₅₀ ^b	Fe	2.92	0.13
	Pd	0.33	0.03

^aReference 32.

^bReference 6. The orbital moment of Fe was calculated with orbital polarization.

bulk Fe and their alloys, which were obtained both experimentally³² and theoretically.⁶ Both orbital and spin magnetic moments of Fe atoms for the Fe₅₀Pt₅₀ alloys are enhanced by a factor of about 1.4 relative to those for bulk Fe. Roughly speaking, MO effects are proportional to the multiplication of the spin and orbital magnetic moments, but not to their sum.¹⁴ Therefore, the increase in both the orbital and spin moments of Fe atoms may be one of the reasons why the ϵ'_{XY} value in the region 4.6–7.8 eV is enhanced by a factor of about 2 in these films.

The remarkable reduction in ϵ'_{XY} at 2.0 eV for the Fe-Pt alloys is probably due to a hybridization-induced modification of the spin-polarized band structure of Fe near to the Fermi energy.¹³ Differences in the ϵ'_{XY} spectra of the ordered and disordered films were observed between disordered and ordered alloy films as shown in Fig. 8. These differences could be essentially related with a change in the electronic structure by an order-disorder phase transition: the fcc crystal structure of a disordered alloy changes into the fct phase of the ordered one by annealing.

It has so far been believed that the magnetic moments of Fe are aligned antiparallel and parallel to those of Pt in ordered and disordered Fe₅₀Pt₅₀ alloys, respectively.¹⁹ However, a recent core-level MCD study has shown that the alignment of the Fe and Pt moments is parallel in Fe₅₁Pt₄₉ films.³¹ Therefore, the change of Ms in Fig. 9(b) does not show any change in the direction of the Pt moments, but suggests some changes in the spin and orbital moments of the Pt and/or Fe atoms.

The magnitude of the dispersion of ϵ'_{XY} centered at ~ 6.3 eV is by about 10% smaller for the ordered film than for the disordered one. This change in ϵ'_{XY} corresponds to that in the Ms for the disordered and ordered alloy films [see Fig. 9(b)]. Therefore, the difference in ϵ'_{XY} is regarded as mainly being due to the change in the Fe moment.

ϵ'_{XY} of the ordered film is by about 50% smaller than that of the disordered one at ~ 3.0 eV. This cannot be explained by a decrease in the Fe moment because the difference is much larger than that of Ms. Many studies have been carried out concerning the change in ϵ'_{XY} in this energy range (2.0–5.0 eV). Weller *et al.* reported that a strong Pt contribution to the Kerr effect was observed at ~ 4.0 eV in Co-Pt alloy systems.^{7,12} Reim *et al.*¹³ argued that the interband contribution of Pd to

ϵ'_{XY} in Fe-Pd alloys shows a simple broad diamagnetic structure centered at 1.9 eV; i.e., the absolute value of ϵ'_{XY} was decreased by Pd substitution at around 1.0 eV. For the Fe-Pt alloy case, Buschow *et al.*⁹ reported that θ_K decreased at around 2.7 eV due to Pt substitution, compared with that of bulk Fe. The orbital moment increases when the crystal symmetry becomes lower during the phase transition from fcc to the fct. Therefore, the decrease in ϵ'_{XY} at 3.0 eV in the ordered film could be due to an increase of the Pt spin and/or orbital moment. The contribution of the increase in the spin and orbital moments of Fe to the MO effects cannot be disregarded in the region between 4.6 and 7.8 eV for Fe-Pt alloy systems. The decrease in the absolute value of ϵ'_{XY} at 3.0 eV in the ordered Fe-Pt alloy could be due to an increase in the spin and/or orbital moment of Pt atoms. Concerning the contribution of polarized Pt, unsettled problems remain and further investigations are required.

V. CONCLUSION

The optical and magneto-optical properties of disordered and ordered Fe₅₁Pt₄₉ films were investigated in the energy range from visible to vacuum ultraviolet. The diagonal and off-diagonal dielectric elements (ϵ_{XX} and ϵ_{XY}) were determined from the results of the optical reflectivity, polar Kerr effect, and magnetic circular dichroism measurements.

The Kerr rotation (θ_K) spectra showed a dispersion-type shape in the 4.6–7.8 eV region for the disordered and ordered films, and were essentially quite similar to that of bulk Fe. The plasma edges were observed at 6.9 eV for the disordered film and at 7.3 eV for the ordered one. ϵ'_{XY} exhibited a dispersion-type spectra centered at 6.3 eV. ϵ''_{XY} showed bell-shaped spectra at around 6.3 eV and a feature of ~ 9.5 eV. The behavior of ϵ'_{XY} for both films were similar to that of bulk Fe from 4.6 to 7.8 eV.

The ϵ'_{XY} dispersion width (centered at 6.3 eV) is about 2.8 eV, which is 1.2 eV wider than that of bulk Fe. The negative peak at 5.2 eV for bulk Fe shifts to 4.8 eV for alloy films. The amplitude of ϵ'_{XY} per Fe atom in the films is about twice that of bulk Fe. Such an enhanced contribution of Fe can be explained by the enhancements of spin and orbital momenta. These results lead to the conclusion that the θ_K enhancement at ~ 4.8 eV can be explained mainly by a decrease in ϵ''_{XX} and the large value of ϵ'_{XY} per Fe atom in the Fe-Pt alloys, but not by the plasma-resonance effect.

The electronic structure of the alloys and the contribution of the Pt moment to the MO effects are still uncertain. Further theoretical and experimental studies are necessary in order to clarify these problems.

ACKNOWLEDGMENTS

The authors wish to thank Dr. S. Yoshida of Electro-technical Laboratory for helpful discussions and Dr. M. Kobayashi, Dr. M. Suzuki, Dr. C. Mitsui, and Dr. Y. Yahata of Science University of Tokyo for their assistance in the reflectivity measurements at the Photon Factory.

- *Present address: Optical Disks Laboratory, Fujitsu Laboratories Ltd., Morinosato-Wakamiya, Atsugi, Kanagawa 243-01, Japan.
- †Present address: National Institute for Advanced Interdisciplinary Research, Tsukuba, Ibaraki 305, Japan.
- ‡Present address: Electrotechnical Laboratory, Tsukuba, Ibaraki 305, Japan.
- ¹P. F. Carcia, A. D. Meinhardt, and A. Suna, *Appl. Phys. Lett.* **47**, 178 (1985).
- ²W. B. Zeper, F. J. A. M. Greidanus, P. F. Carcia, and C. R. Fincher, *J. Appl. Phys.* **65**, 4971 (1989).
- ³S. Hashimoto, Y. Ochiai, and K. Aso, *Jpn. J. Appl. Phys.* **28**, L1824 (1989).
- ⁴K. Nakamura, S. Tsunashima, S. Iwata, and S. Uchiyama, *IEEE Trans. Magn.* **MAG-25**, 3758 (1989).
- ⁵T. Sugimoto, T. Katayama, Y. Suzuki, and Y. Nishihara, *Jpn. J. Appl. Phys.* **28**, L2333 (1989).
- ⁶G. H. O. Daalderop, P. J. Kelly, and M. F. H. Schuurmans, *Phys. Rev. B* **44**, 12 054 (1991).
- ⁷D. Weller and W. Reim, *Appl. Phys. A* **49**, 599 (1989).
- ⁸T. Sugimoto, T. Katayama, M. Hashimoto, Y. Suzuki, and Y. Nishihara, *J. Magn. Soc. Jpn.* **15**, 419 (1991); T. Katayama, T. Sugimoto, Y. Suzuki, M. Hashimoto, P. de Haan, and J. C. Lodder, *J. Magn. Magn. Mater.* **104-107**, 1002 (1992); T. Sugimoto, T. Katayama, Y. Suzuki, M. Hashimoto, Y. Nishihara, A. Itoh, and K. Kawanishi, *ibid.* **104-107**, 1845 (1992).
- ⁹K. H. J. Buschow, P. G. van Engen, and R. Jongebreur, *J. Magn. Magn. Mater.* **38**, 1 (1983).
- ¹⁰E. R. Moog, J. Zak, and S. D. Bader, *J. Appl. Phys.* **69**, 880 (1991); **69**, 4559 (1991).
- ¹¹K. Sato, H. Hongu, H. Ikekame, J. Watanabe, K. Tsuzukiya, Y. Togami, M. Fujisawa, and T. Fukuzawa, *Jpn. J. Appl. Phys.* **31**, 3603 (1992).
- ¹²D. Weller, W. Reim, K. Spörl, and H. Brändle, *J. Magn. Magn. Mater.* **93**, 183 (1991).
- ¹³W. Reim, H. Brändle, D. Weller, and J. Schoenes, *J. Magn. Magn. Mater.* **93**, 220 (1991).
- ¹⁴P. N. Argyres, *Phys. Rev.* **97**, 334 (1955).
- ¹⁵Y. Wu, J. Stöhr, B. D. Hermsmeier, M. G. Samant, and D. Weller, *Phys. Rev. Lett.* **69**, 2307 (1992).
- ¹⁶J. W. Cable, E. O. Wollan, and W. C. Koehler, *Phys. Rev.* **138**, A755 (1965).
- ¹⁷J. L. Erskine, *Phys. Rev. Lett.* **37**, 157 (1976).
- ¹⁸L. Grafu, A. Kussmann, and M. Fallot, *Ann. Phys.* **10**, 291 (1938).
- ¹⁹A. Z. Men'shikov, Yu. A. Dorofeyev, V. A. Kazantsev, and S. K. Sidoror, *Fiz. Metal. Metalloved.* **38**, 505 (1974).
- ²⁰T. Koide, S. Sato, H. Fukutani, H. Noda, S. Suzuki, T. Hanyu, T. Miyahara, S. Nakai, I. Nagakura, A. Kakizaki, H. Maezawa, T. Ohta, and T. Ishii, *Nucl. Instrum. Math. A* **239**, 350 (1985).
- ²¹T. Koide, T. Shidara, and H. Fukutani, *Rev. Sci. Instrum.* **63**, 1462 (1992); T. Koide, T. Shidara, H. Fukutani, K. Yamaguchi, A. Fujimori, S. Kimura, T. Sugimoto, T. Katayama, and Y. Suzuki, *ibid.* **63**, 1371 (1992).
- ²²P. M. Oppeneer, T. Maurer, J. Sticht, and J. Kübler, *Phys. Rev. B* **45**, 10 924 (1992).
- ²³A. Seignac and S. Robin, *Solid State Commun.* **11**, 217 (1972).
- ²⁴For example, W. Reim and J. Schoenes, in *Ferromagnetic materials*, edited by K. H. J. Buschow and E. P. Wohlfarth (North-Holland, Amsterdam, 1990), Vol. 5, Chap. 2, pp. 137-147.
- ²⁵F. Wooten, *Optical Properties of Solids* (Academic, New York, 1972), pp. 244-250.
- ²⁶P. B. Johnson and R. W. Christy, *Phys. Rev. B* **9**, 5056 (1974).
- ²⁷M. Hayashi, T. Katayama, Y. Suzuki, M. Taninaka, A. Thia-ville, and W. Geerts, in *Proceedings of the 1st International Symposium on Metallic Multilayers '93 Kyoto, Japan* [*J. Magn. Magn. Mater.* (to be published)].
- ²⁸H. Feil and C. Hass, *Phys. Rev. Lett.* **58**, 65 (1987).
- ²⁹G. G. Low, *Adv. Phys.* **18**, 371 (1968).
- ³⁰H. Ebert and H. Akai, *J. Appl. Phys.* **67**, 4798 (1990).
- ³¹T. Koide *et al.* (unpublished).
- ³²R. A. Reck and D. L. Fry, *Phys. Rev.* **184**, 492 (1969).